Published in final edited form as:
Gastroenterology. 2013 February ; 144(2): 294–297. doi:10.1053/j.gastro.2012.10.030.

Optical Imaging of Periostin Enables Early Endoscopic Detection and Characterization of Esophageal Cancer in Mice

Gabrielle S. Wong[1,2,4], **Peiman Habibollahi**[8], **Pedram Heidari**[8], **Ju-Seog Lee**[7], **Andres J. Klein-Szanto**[6], **Todd J. Waldron**[1,2,4], **Phyllis Gimotty**[4,5], **Hiroshi Nakagawa**[1,2,4], **Philip R. Taylor**[11], **Timothy C. Wang**[9,10], **Umar Mahmood**[8], and **Anil K. Rustgi**[1,2,3,4]

[1]) Division of Gastroenterology, University of Pennsylvania Perelman School of Medicine, Philadelphia, PA, 19104, USA

[2]) Department of Medicine, University of Pennsylvania Perelman School of Medicine, Philadelphia, PA, 19104, USA

[3]) Department of Genetics, University of Pennsylvania, Philadelphia, PA, 19104, USA

[4]) Abramson Cancer Center, University of Pennsylvania, Philadelphia, PA, 19104, USA

[5]) Division of Biostatistics, Center for Clinical Epidemiology and Biostatistics, University of Pennsylvania, Philadelphia, PA, 19104, USA

[6]) Department of Pathology and Cancer Biology Program, Fox Chase Cancer Center, Philadelphia, PA, 19104, USA

[7]) Department of Systems Biology, MD Anderson Cancer Center, Houston, TX, 77030, USA

[8]) Division of Nuclear Medicine and Molecular Imaging, Department of Radiology, Massachusetts General Hospital, Boston, MA, 02114, USA

[9]) Division of Digestive and Liver Diseases, Department of Medicine, Columbia University Medical Center, New York, NY, 10032, USA

[10]) Herbert Irving Comprehensive Cancer Center, Columbia University Medical Center, New York, NY, 10032, USA

[11]) Genetic Epidemiology Branch, DCEG, NCI, NIH, Bethesda, MD 20892, USA

Abstract

Imaging strategies that detect early-stage esophageal squamous cell carcinoma (ESCC) could improve clinical outcomes, combined with endoscopic approaches. Periostin is an integrin-binding protein that is important in the tumor microenvironment. We created a fluorescent-labeled

Corresponding Author: Anil K. Rustgi, MD T. Grier Miller Professor of Medicine & Genetics Chief of Gastroenterology 600 CRB University of Pennsylvania 415 Curie Blvd. Philadelphia, PA 19104 215-898-0154 FAX: 215-573-5412 anil2@mail.med.upenn.edu.

Authorship note: Gabrielle S. Wong and Peiman Habibollahi contributed equally to this work.

Conflict of Interest: The authors have declared that no conflicts of interest exist.

Contributions G.S.W. and P.H. performed the experiments and data analysis with assistance from P.H, T.J.W., HN and P.G. J.S.L carried out bioinformatic analyses and T.J.W. and A.K.S. performed histopathological analyses. P.R.T. provided gene expression microarray data from matched primary ESCC samples. G.S.W and A.K.R designed and conceived this study. U.M. and A.K.R supervised this work with help from T.C.W. The manuscript was written by G.S.W, P.H., U.M and A.K.R.

antibody that recognizes periostin and binds specifically to ESCC xenograft tumors in mice. In *L2-cre;p120ctnLoxP/LoxP* mice, which develop squamous cell cancers that resemble human ESCC, we visualized the probe in preneoplastic and neoplastic esophageal lesions using near-infrared fluorescent imaging with upper gastrointestinal endoscopy. Periostin might be a biomarker of the esophageal tumor microenvironment that can be used to detect preneoplastic lesions.

Keywords

mouse model; neoplasm; extracellular matrix; *POSTN*

Esophageal cancer is the sixth leading cause of cancer-related deaths worldwide[1]. Esophageal cancer is comprised of two major subtypes: esophageal adenocarcinoma (EAC) and esophageal squamous cell carcinoma (ESCC). ESCC is the predominant subtype found in developing countries and is associated with high mortality rates due to late diagnosis, frequently presenting at advanced stages of disease where metastasis has occurred[2, 3]. Therefore, early detection methods to identify lesions with high grade dysplasia or carcinoma *in situ* in the esophageal mucosa are needed in order to employ interventional therapies to prevent cancer progression and improve patient survival. Current screening modalities include endoscopic and non-endoscopic screening such as white-light (WL) endoscopy with Lugol's iodine staining and esophageal balloon cytology, respectively[4]. Recent studies have demonstrated the translational potential of coupling molecular biomarkers associated with cancer with novel, sensitive imaging technologies as a means for the early diagnosis of esophageal cancer[5, 6].

We had established previously a tumor invasion gene signature derived from mRNA profiling of invading genetically engineered human esophageal cells, transformed with epidermal growth factor receptor (EGFR) overexpression and $p53^{R175H}$ mutation, (EPC2-hTERT-EGFR-$p53^{R175H}$) that was grown in a 3D organotypic culture (OTC) system[7]. Expression of 491 genes (tumor invasion gene signature) was significantly ($P < 0.001$ and 3-fold) different between invading versus non-invading EPC2-hTERT-EGFR-$p53^{R175H}$ cells grown in OTC[7]. Therein, we sought to examine the prognostic relevance of the tumor invasion gene signature in human ESCC by using gene expression data from Shanxi Cancer Hospital in China of matched ESCC tumors (Shanxi cohort, $n = 53$)[8]. ESCC patients in the Shanxi cohort were stratified according to the absence or presence of the tumor invasion signature with use of the support vector machine (SVM) algorithm (Figure 1A). Kaplan-Meier plots in the Shanxi cohort showed that ESCC patients with the tumor invasion signature have significantly shorter overall survival (OS) ($p = 0.049$, by log-rank test) than those without the presence of the tumor invasion signature (Figure 1B).

We have established recently that periostin is the highest upregulated protein in our tumor invasion gene signature for ESCC as well as an important mediator of tumor invasion within the microenvironment[7]. Immunohistochemical analysis of an ESCC tissue microarray revealed increasing periostin expression with advancing ESCC progression[7]. Periostin is a secreted matricellular protein that binds to a variety of proteins within the extracellular matrix (ECM) such as fibronectin and tenascin C[9] and activates signaling pathways that are important in cell adhesion and motility[10–13]. Periostin is dynamically expressed during embryonic development but has low basal expression in adult connective tissues such as periosteum and aortic valves[13]. Wound injury, inflammation, fibrosis and cancer lead to re-induction of periostin[13]. Interestingly, periostin is significantly upregulated in a large gene expression dataset of human ESCC tumors (Shanxi cohort) compared to their matched normal control tissues and this upregulation of periostin was similar to periostin expression

levels found in the invading EPC2-hTERT-EGFR-p53^{R175H} cells compared to non-invading EPC2-hTERT-EGFR-p53^{R175H} cells, indicating that periostin plays a key role in ESCC development (Figure 1C). We also evaluated periostin expression in a panel of ESCC cell lines (Figure 1D).

We have developed the first *in vivo* imaging biomarker for periostin through the conjugation and purification of a polyclonal periostin antibody which detects all four isoforms of periostin, with a near infra-red fluorochrome (Cy 5.5). The probe was intravenously injected into athymic nude mice bearing tumor xenografts of two independent ESCC cell lines (TE-11 and TT). Fluorescent imaging showed a strong fluorescent signal in TE-11 xenograft tumors expressing periostin (Figure 1E, left panel, white arrow) compared to a low fluorescent signal in TT xenograft tumors (Figure 1E, right panel, white arrow), which do not express periostin. The optical probe displayed a significantly high target to background ratio (TBR) in TE-11 xenograft tumors compared to TT xenograft tumors (Figure 1F). Since periostin is a secreted protein found in connective tissues, there is expected background signal observed in the sternum (Figure 1E, right panel, black arrowhead) as well as expected excretion of fluorochrome in the bladder (Figure 1E, right panel, black arrow). The specificity of the periostin optical probe was established in additional studies (Supplementary Figure 1A–C). We found that the incubation of the blocking, unlabeled antibody with the periostin optical probe led to markedly decreased fluorescent signal that is similar to the negative control (Supplementary Figure 1D).

We have characterized a genetic mouse model of ESCC by conditionally deleting the cell adhesion molecule p120 catenin (*p120ctn*) specifically in the squamous oral cavity, esophagus and forestomach (*L2-cre;p120ctn$^{LoxP/LoxP}$*) that recapitulates the temporal progression of human ESCC[14]. There is increased periostin expression in the sera of mice with severe dysplasia compared to mice with mild dysplasia and control mice (Figure 2A and 2B).

We next performed upper gastrointestinal (GI) endoscopies in the three cohorts of mice using a novel custom multispectral endoscopy system capable of both WL and near infra-red (NIR) imaging and utilizing the periostin optical probe. Strikingly, we observed the highest NIR fluorescent signal in the mice with severe dysplasia (Figure 2C, bottom middle panel) compared to less NIR signal in mice with mild dysplasia (Figure 2C, middle panel) and no NIR fluorescent signal in control mice (Figure 2C, upper middle panel). Moreover, the overlay of WL and NIR images of mice with severe dysplasia displayed upregulation of periostin fluorescent expression localized in lesions observed in the WL image (Figure 2C, bottom left panel, Figure 2D) compared to no periostin expression detected in control mice (Figure 2C, upper right panel, Figure 2D). Intriguingly, there was a slight increase in periostin fluorescent expression observed in mice with mild dysplasia despite lack of macroscopic lesions detected in WL image (Figure 2C, middle left panel, Figure 2D) compared to control mice (Figure 2D), suggesting that periostin may be sensitive tool to detect neoplastic lesions before they are identified by conventional WL endoscopy. Hispathological examination of esophagi from mice in these three groups confirmed mild squamous dysplasia in *L2-cre; p120ctn$^{LoxP/LoxP}$* mice (Figure 2E, middle panel, Supplementary Figure 2B) and severe dyplastic areas in older *L2-cre; p120ctn$^{LoxP/LoxP}$* mice (Figure 2E, bottom panel, Supplementary Figure 2C). Immunohistochemical analysis of periostin expression in the esophagi of mice from the above three cohorts, revealed increasing periostin expression with advancing stages of dysplasia (Supplementary Figure 3A–C). Thus periostin has the potential to serve as a biomarker for early ESCC detection through innovative optical imaging.

The imaging platforms we have created result in the quantification of the fluorescent signal[15], allowing mapping of probe signal intensity with periostin levels in the tumor ECM. There is no known toxicity from cyanine fluorochromes at the levels administered for optical imaging. Thus, the methods developed here are translatable for human use and could provide an adjunct to standard WL endoscopy as it is currently employed.

Supplementary Material

Refer to Web version on PubMed Central for supplementary material.

Acknowledgments

This work was supported by NIH/NCI P01-CA098101, NIH T32-CA115299, NIH/NCI U01-CA14305603, NIH/NIDDK Center for Molecular Studies in Digestive and Liver Diseases (P30-DK050306), American Cancer Society (RP-10-033-01-CCE) and the Intramural Research Program of the US National Institutes of Health, NCI and the Division of Cancer Epidemiology and Genetics. We acknowledge the Molecular Pathology and Imaging Core, Molecular Biology/Gene Expression Core, Cell Culture Core and Mouse Core. We are grateful to other members of the Rustgi lab for helpful discussions.

References

1. Ferlay J, et al. Int J Cancer. 2010; 127:2893–917. [PubMed: 21351269]
2. Mayer P, et al. The New England Journal of Medicine. 2003:2241–52. [PubMed: 14657432]
3. Wang LS, et al. Am J Gastroenterol. 1999; 94:1933–40. [PubMed: 10406262]
4. Lao-Sirieix P, et al. Nat Rev Clin Oncol. 2012; 9:278–87. [PubMed: 22430857]
5. Bird-Lieberman EL, et al. Nat Med. 2012; 18:315–21. [PubMed: 22245781]
6. Habibollahi P, et al. Theranostics. 2012; 2:227–34. [PubMed: 22400064]
7. Michaylira CZ, et al. Cancer Res. 2010; 70:5281–92. [PubMed: 20516120]
8. Su H, et al. Clin Cancer Res. 2011; 17:2955–66. [PubMed: 21385931]
9. Kudo A. Cell Mol Life Sci. 2011; 68:3201–7. [PubMed: 21833583]
10. Horiuchi K, et al. J Bone Miner Res. 1999; 14:1239–49. [PubMed: 10404027]
11. Maruhashi T, et al. J Biol Chem. 2010; 285:13294–303. [PubMed: 20181949]
12. Butcher JT, et al. Dev Biol. 2007; 302:256–66. [PubMed: 17070513]
13. Ruan K, et al. Cell Mol Life Sci. 2009
14. Stairs DB, et al. Cancer Cell. 2011; 19:470–83. [PubMed: 21481789]
15. Upadhyay R, et al. Radiology. 2007; 245:523–31. [PubMed: 17940307]

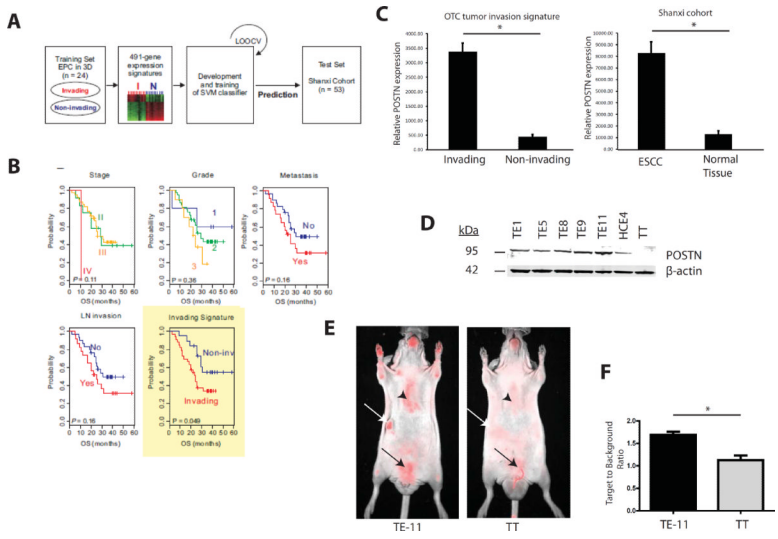

FIGURE 1. Periostin is upregulated in invasive human ESCC

A. Schematic of prediction models constructed for evaluation of predicted outcomes based on gene expression signatures.

B. Kaplan-Meier plots of the overall survival (OS) of the two predicted groups of patients. The differences between groups were significant, as indicated by the log-rank test.

C. Comparison of relative periostin (*POSTN*) expression in gene expression dataset comparing invading versus non-invading EPC2-hTERT-EGFR-p53^{R175H} cells grown in OTC to periostin expression in gene expression dataset of matched ESCC tumors in Shanxi cohort. Error bars represent +/− SEM. *p<0.05

D. Immunoblot of POSTN (95 kDa) expression in panel of ESCC cell lines. β-actin was used as a loading control.

E. Fluorescent images of periostin optical probe injected into nude mice bearing tumor xenografts of TE-11 and TT (white arrows). TT tumor xenografts were used as a negative control. Sternum is indicated by black arrowheads and bladder is indicated with black arrows.

F. Quantification of fluorescent signal from the periostin optical probe detected from TE-11 and TT tumor xenografts (n=5 from each group). Bar graphs represent target-to-background ratios (TBR) +/− SEM *p<0.05. Note that background TBR=1 implies no increased probe uptake in tumor relative to background tissue.

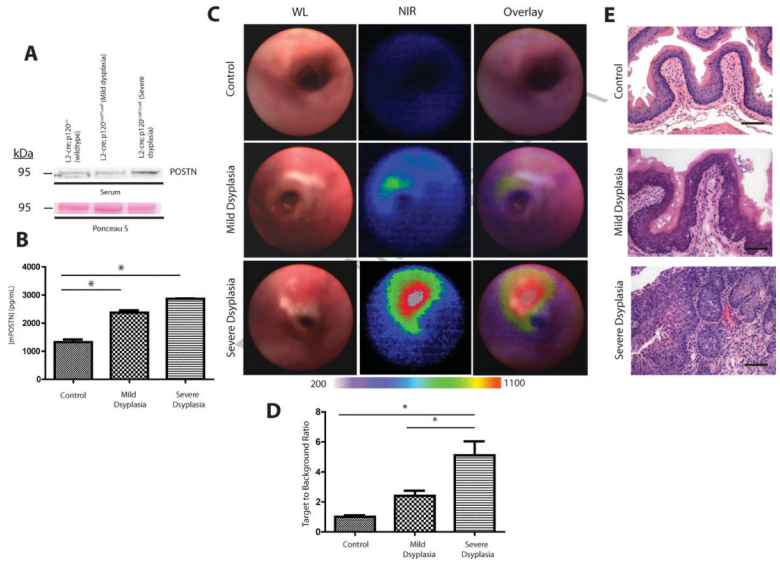

FIGURE 2. Periostin expression is detected with increasing ESCC progression in genetic mouse model of ESCC

A. Immunoblot of periostin expression in mouse sera from three cohorts of mice at different stages of disease: control *L2-cre; p120ctn*$^{LoxP/+}$, *L2-cre; p120ctn*$^{LoxP/LoxP}$ with mild dysplasia and *L2-cre; p120ctn*$^{LoxP/LoxP}$ with severe dysplasia (n=6 mice from each group). Ponceau S staining of immunoblot was performed as loading control.

B. ELISA of periostin levels present in mouse sera from the above three cohorts of mice. (n=6 mice from each cohort). Error bars represent +/− SEM *p<0.05

C. Representative white light (WL), near infra-red (NIR) and overlay images from upper GI endoscopies in mice from the above three cohorts. Color map represents range of fluorescent signal intensities (200–1100) in images.

D. Quantification of fluorescent signal from periostin optical probe detected from upper GI endoscopies in mice from the above three cohorts (n=3 from each cohort). Bar graphs represent TBR +/− SEM *p<0.05

E. Histopathological analysis of representative esophagi isolated from mice from the above three cohorts in top to bottom panels. Scale bars are 100 μM.